Hierarchical Multimodal Mesoporous Carbon Materials with Parallel Macrochannels

Bao-Lian Su,*,† Aurélien Vantomme,† Lidwine Surahy,† René Pirard,‡ and Jean-Paul Pirard‡

Laboratoire de Chimie des Matériaux Inorganiques (CMI), The University of Namur (FUNDP), 61 rue de Bruxelles, B-5000 Namur, Belgium, and Laboratoire de Génie Chimique, Institut de Chimie (Bât. B6a), Université de Liège, B-4000 Liège, Belgium

Received January 31, 2007. Revised Manuscript Received April 9, 2007

Hierarchically structured multimodal meso-macroporous carbon materials have been prepared by using the nanoreplication of the mesoporous walls of a meso-macroporous zirconia exotemplate. Like the zirconia exotemplate, the pure carbon material possesses funnel shaped straight macrochannels, parallel to each other and perpendicular to the tangent of the particles' dense mesoporous shell. As a result of the funnel-like shape, each macrochannel has a pore size gradient with a large opening centered at 300−700 nm. The walls of the macrochannels and the dense mesoporous shells are formed by a hierarchical mesostructured porous system with uniform mesopore sizes centered at 3, 15−17, and 25−50 nm. Macrochannels are interconnected with hierarchically mesostructured walls and shells. A high surface area of 950 m^2/g with a mesopore volume of 0.44 cm^3/g is obtained. The possibility of the nanoreplication of other meso-macroporous oxides such as aluminosilicates, titania, and niobium oxide with different macrochannel size, shape, and organization has also been studied to generate meso-macroporous carbon materials with different organizations of the macrochannels.

1. Introduction

Porous carbons are promising candidates for use in a wide range of applications, including water and air purification, adsorption, catalysis, electrodes, and energy storage,[1,2] as a result of their high surface areas, large pore volume, chemical inertness, and excellent mechanical stability. The most promising way to prepare two- or three-dimensional porous carbon materials with well-defined structural, textural, and morphological properties is the exotemplating method.[3] In this approach, a suitable template is impregnated with a carbon precursor, which is subsequently carbonized under non-oxidizing conditions. After removal of the template, typically by dissolution, a negative carbon replica of the starting template is obtained. There have been many studies devoted to the preparation of carbon materials with different pore sizes and structures by using various exotemplates such as alumina membranes,[4,5] zeolites,[6−8] siliceous opals,[9,10] silica xerogels,[11] and mesoporous silicas (MCM-48,[12−14] SBA-15,[15] MSU-H,[16] MSU-1[17]). Another promising strategy was recently[016] developed by Zhao et al.,[18−22] which led to the preparation of highly structured so-called "true mesoporous carbons". FDU-14[22] crystallizes in a space group of $Ia\bar{3}d$ similar to KIT-6[23] and MCM-48,[24] FDU-15[22] crystallizes in a space group of *P6m* similar to SBA-15,[25] and FDU-16[22] crystallizes in a space group of $Im\bar{3}m$ similar to SBA-16 with interconnected cages.[26] Compared to the nanocasting method, the synthesis route developed by Zhao et al.[18−22] on the basis of the organic−organic interaction between a thermopoly-

* Corresponding author. E-mail: bao-lian.su@fundp.ac.be. Fax: +32-81-725414.
† The University of Namur.
‡ Université de Liège.

(1) Foley, H. C. *Microporous Mater.* **1995**, *4*, 407.
(2) Kyotani, T. *Carbon* **2000**, *38*, 269.
(3) Schüth, F. *Angew. Chem., Int. Ed.* **2003**, *42*, 3604−3622.
(4) Che, G.; Lakshmi, B. B.; Fisher, E. R.; Martin, C. R. *Nature* **1998**, *393*, 346−349.
(5) Kyotani, T.; Tsai, L.; Tomita, A. *Chem. Mater.* **1995**, *7*, 1427.
(6) Kyotani, T.; Nagai, T.; Inoue, S.; Tomita, A. *Chem. Mater.* **1997**, *9*, 609.
(7) Ma, Z.; Kyotani, T.; Tomita, A. *Chem. Commun.* **2000**, 2365.
(8) Ma, Z.; Kyotani, T.; Tomita, A. *Chem. Mater.* **2001**, *13*, 4413.
(9) Zakhidov, A. A.; Baughman, R. H.; Iqbal, Z.; Cui, C.; Khayrullin, I.; Dantas, S. O.; Marti, J.; Ralchenko, V. G. *Science* **1998**, *282*, 897.
(10) Stein, A. *Microporous Mesoporous Mater.* **2001**, *44−45*, 227.
(11) Fuertes, A. B. *Chem. Mater.* **2004**, *16*, 449.
(12) Kruk, M.; Jaroniec, M.; Ryoo, R.; Joo, S. H. *J. Phys. Chem. B* **2000**, *104*, 7960.
(13) Joo, S. H.; Jun S.; Ryoo, R. *Microporous Mesoporous Mater.* **2001**, *44−45*, 153.
(14) Joo, S. H.; Choi, S. J.; Oh, I.; Kwak, J.; Liu, Z.; Terasaki, O.; Ryoo, R. *Nature* **2001**, *412*, 169.
(15) Jun, S.; Joo, S. H.; Ryoo, R.; Kruk, M.; Jaroniec, M.; Liu, Z.; Ohsuma, T.; Terasaki, O. *J. Am. Chem. Soc.* **2000**, *122*, 10712.
(16) Kim, S. S.; Pinnavaia, T. S. *Chem. Commun.* **2001**, 2418.
(17) Alvarez, S.; Fuertes, A. B. *Carbon* **2004**, *42*, 433.
(18) Meng, Y.; Gu, D.; Zhang, F.; Shi, Y.; Yang, H.; Li, Z., Yu, C.; Tu, B.; Zhao, D. *Angew. Chem., Int. Ed.* **2005**, *44*, 2
(19) Zhang, F. Q.; Meng, Y.; Gu, D.; Yan, Y.; Yu, C. Z.; Tu, B.; Zhao, D. Y. *J. Am. Chem. Soc.* **2005**, *127*, 13508.
(20) Zhao, D. Y.; Yan, Y.; Tu, B.; Yang, H. F. *Small* **2007**, *3*, 198.
(21) Huang, Y.; Cai, H. Q.; Yu, T.; Zhang, F. Q.; Zhang, F.; Meng, Y.; Gu, D.; Wan, Y.; Sun, X. L.; Tu, B.; Zhao, D. Y. *Angew. Chem., Int. Ed.* **2007**, *46*, 1089.
(22) Meng, Y.; Gu, D.; Zhang, F. Q.; Shi, Y. F.; Cheng, L.; Feng, D.; Wu, Z. X.; Chen, Z. X.; Wan, Y.; Stein, A. Zhao, D. Y. *Chem. Mater.* **2006**, *18*, 4447.
(23) Kleitz, F.; Choi, S. H.; Ryoo, R. *Chem. Commun.* **2003**, 2136.
(24) Kresge, C. T.; Leonowicz, M. E.; Roth, W. J.; Vartuli, J. C.; Beck, J. S. *Nature* **1992**, *359*, 710.
(25) Zhao, D.; Feng, J.; Huo, Q.; Melosh, N.; Frederickson, G. H.; Chemlka, B. F.; Stucky, G. D. *Science* **1998**, *279*, 548.
(26) Zhao, D.; Huo, Q.; Feng, J.; Chmelka, B. F.; Stucky, G. D. *J. Am. Chem. Soc.* **1998**, *120*, 6024.

10.1021/cm070294o CCC: $37.00
Published on Web 05/27/2007

merizable polymer (carbon precursor) and the copolymer triblock (P123 and F127) as surfactant molecules leads directly to porous carbon materials after the carbonization in an inert atmosphere at 350 °C and followed by pyrolysis at 900 °C.

Recently the carbon materials with a hierarchical pore system have attracted much interest owing to potential technological applications.[27] A multi-scaled pore system has obvious advantages over the unimodal pore size of other carbon materials in terms of diffusion efficiency, accessibility to the pores by guest species, and large porous volumes.[28] Meso-macroporous carbon materials have thus been synthesized using a meso-macroporous silica with a spong-like structures as an exotemplate.[29−31] Chai et al.[32] have synthesized macroporous carbons with mesoporous walls by template replication of small silica particle aggregates. The aggregates themselves had been templated by a self-assembly process that employed an ordered lattice of larger, monodispersed polystyrene spheres as a mold. Kim et al.[33] reported that an interconnected macroporous−mesoporous carbon could be targeted by using a removable template composed of monodispersed silica particles and a silica network that had been polymerized in situ. Stein et al.[34] developed a new methodology of assembling integrated multifunctional porous materials: titania coated three-dimensionally ordered macroporous (3DOM) carbons. 3DOM carbon was synthesized from a resorcinol-formaldehyde (RF) sol−gel carbon precursor, using poly(methyl methacrylate) (PMMA) colloidal crystals as templates followed by the decomposition of PMMA and the pyrolysis of the carbon precursor. Lindén et al.[29−31] demonstrated another facile preparation of nanocasted carbon monoliths exhibiting a multimodal hierarchical pore network. However, to improve the performance of these macro-mesoporous materials when used in selective membranes, catalyst supports, molecular separators, and biological-cell sensors, an ordered network of macrochannels is required rather than the large pore cells or sponge-like macroporous structures or macrovoids formed between carbon cyclinders. Despite many efforts,[4,5] the fabrication of bimodal porous carbon membranes, composed of straight, well-aligned channels with mesoporous walls, still remains a great technical challenge. To date, the preparation strategies developed on the basis of a template replication process do not yield such sophisticated structures because of the lack of a suitable template coupled with the fact that the product obtained by template replication is always the exact replica of the template. The direct synthesis strategy which was recently developed yields only the unimodal mesoporous carbon materials.[18−22]

It has recently been reported that hierarchically structured meso-macroporous metal oxides (silicoaluminates,[35−39] Al_2O_3,[37−40] ZrO_2,[37−43] TiO_2,[37−44] Y_2O_3,[37−44] Nb_2O_5,[37−44] and mixed oxides[37−44]) possessing well ordered funnel-like macrochannels with mesoporous walls can be targeted via a "one-pot" self-formation process. Their synthesis is quite simple and is performed on the basis of the chemistry of metal alkoxides. A comprehensive study following the formation of the funnel-like macrochannels has recently been completed. Optical microscopy was used in situ to follow the reaction and has revealed that these hierarchically structured meso-macroporous metal oxides are produced by a self-formation mechanism.[37−39] The key point of this novel synthesis process is the very high rate at which the metal alkoxides hydrolyzed undergo condensation reactions in aqueous solution. Alcohol molecules can be generated suddenly as soon as the metal alkoxide precursor is in contact with the water molecules. The molecules of alcohol will increase in quantity as the reaction progresses because one metal alkoxide molecule can produce at least two more alcohol molecules. These alcohol molecules can be considered as the "porogene" in the generation of the funnel-like macrochannels with hierarchically mesostructured porous walls. This new process could be of great interest and is a significant advance toward the understanding of the formation mechanism of these hierarchically structured porous materials. This process could be adopted for the large scale preparation of the mesoporous membranes with well-oriented, funnel-like, straight macrochannels which interconnect with the mesoporous shell and pore walls. The process could be used to targeted new functional materials with very sophisticated architectures. Instead of alcohol molecules as the self-generated "porogene", it is possible to imagine other precursors which can generate and release "porogene molecules" in liquid and even in gas form. The formation mechanism of these meso-macroporous structures has been discussed in depth in recent papers.[37−39] These metal oxides with a hierarchical meso-macroporous network have additional benefits as a result of the enhanced access to the mesopores by the regular macrochannel array.

Owing to the excellent performance of carbon materials in applications involving both hydrogen and energy storage, one must ask whether this simple process for the preparation of meso-macroporous metal oxides can be employed to produce carbon materials with similar porous networks. Currently, there is no known direct method that can produce these sophisticated hierarchical structures with pure carbon. Nanoreplication could be the unique strategy, and thus the

(27) Lee, J.; Han, S.; Hyeon, T. *J. Mater. Chem.* **2004**, *14*, 478.
(28) Su, F.; Zhao, X. S.; Wang, Y.; Zeng, J.; Zhou, Z.; Lee, J. Y. *J. Phys. Chem. B* **2005**, *109*, 20200.
(29) Taguchi, A.; Smatt, J. H.; Lindén, M. *Adv. Mater.* **2003**, *15*, 1209.
(30) Lu, A. H.; Smatt, J. H.; Backlund, S.; Lindén, M. *Microporous Mesoporous Mater.* **2004**, *72*, 59.
(31) Lu, A. H.; Smatt, J. H.; Lindén, M. *Adv. Funct. Mater.* **2005**, *15*, 865.
(32) Chai, G. S.; Shin, I. S.; Yu, J. S. *Adv. Mater.* **2004**, *16*, 22.
(33) Kim, P.; Joo, S. B.; Kim, W.; Kong, S. K.; Song, I. K.; Yi, J. *Carbon* **2006**, *44*, 381−392.
(34) Wang, Z. Y.; Ergang, N. S.; Al-Daous, M. A.; Stein, A. *Chem. Mater.* **2005**, *17*, 6805.
(35) Léonard, A.; Blin J. L.; Su, B. L. *Chem. Commun.* **2003**, 2568.
(36) Léonard, A.; Su, B. L. *Chem. Commun.* **2004**, 1674
(37) Léonard, A.; Su, B. L. *Colloids Surf., A* **2007**, *300*, 129.
(38) Vantomme, A.; Leonard, A.; Yuan, Z. Y.; Su, B. L. *Colloids Surf., A* **2007**, *300*, 70.
(39) Vantomme, A.; Leonard, A.; Yuan Z. Y.; Su, B. L. *Key Eng. Mater.* **2007**, *336−338*, 1933
(40) Ren, T. Z.; Yuan, Z. Y.; Su, B. L. *Langmuir* **2004**, *20*, 1674.
(41) Blin, J. L.; Léonard, A.; Gigot, L.; Yuan, Z. Y.; Vantomme, A.; Cheetham, A. K.; Su, B. L. *Angew. Chem., Int. Ed.* **2003**, *42*, 2872.
(42) Yuan, Z. Y.; Vantomme, A.; Léonard A.; Su, B. L. *Chem. Commun.* **2003**, 1558.
(43) Vantomme, A.; Yuan, Z. Y.; Su, B. L. *New J. Chem.* **2004**, *28*, 1083.
(44) Yuan, Z. Y.; Ren, T. Z.; Vantomme, A.; Su, B. L. *Chem. Mater.* **2004**, *10*, 5096.

resulting metal oxides with meso-macroporous architectures and straight macrochannels could promise ideal templates for the fabrication of meso-macroporous carbon materials. However, the great challenge here is how to preserve the macrochannels in the replica of such a macrochanneled template because the conventional template replication strategy generates only the exact replica of the template. The macrochannels present in the template can thus be lost and would not be transmitted to the final materials. Therefore, a suitable strategy of nanoreplication must be used.

This present work describes the preparation of hierarchically structured meso-macroporous carbon possessing aligned and uniformly sized macrochannels with interconnected, well-organized, wormhole-like hierarchically porous walls with mesoporosities centered at 3, 10−17, and 25−50 nm. Here, the template replication of micro-meso-macroporous zirconia as a host scaffold is illustrated as an example. Results using other metal oxides as exotemplates are also discussed. The present work gives a concrete example for the preparation of hierarchical multimodal porous nitrides, silicates, and even SiC. The reason why we did not use the hierarchically meso-macroporous siliceous materials is due to the lack of such hierarchically porous silicas. In fact, as a result of the low reactivity (thus the slow rates of hydrolysis and polycondensation) of alkoxysilanes, it proved impossible to synthesize suitable meso-macroporous silica materials for use as exotemplate possessed mesoporous walls around the funnel-like straight macrochannels employing the self-formation process described without any hard external template in spite of our important efforts. Thus an alternative exotemplate based on ZrO_2 had to be employed.

2. Experimental Section

2.1. Synthesis. *2.1.1. Exotemplates.* The starting multimodal meso-macroporous zirconia exotemplate CMI-7-Zr was easily prepared by a self-generation process previously reported elsewhere.[37−39] Zirconium *n*-propoxide ($[Zr(OC_3H_7)_4]$, 70 wt % in 1-propanol) was added dropwise to an aqueous solution with a controlled pH value. The self-formation procedure took place immediately. The pH value was adjusted, which is dependent on the chain length of alkoxide to ensure a high hydrolysis and polycondensation rate in aqueous solution. The obtained mixture was then transferred into a Teflon lined autoclave and heated under static conditions at 60 °C for 48 h. The product was filtered, washed, and dried. This very simple procedure can be applied to any metal alkoxides and with the above information; the process can easily be reproduced, and no more information can be given.

2.1.2. Multimodal Meso-Macroporous Carbon. Impregnation and carbonization experiments were performed with a defined amount of sucrose per zirconia exotemplate; subsequently, this amount was optimized to improve the efficiency of our replication method. As described in the introduction, the conventional template replication strategy generates only the exact replica of the template, and the macrochannels present in the template can thus disappear and would therefore not be transmitted to the final materials. The conventional nanoduplication strategy has to be modified such that only the mesopores are filled while the macrochannels of exotemplate remain empty. Hence, the quantity of sucrose introduced was carefully controlled on the basis of the mesoporous volumes of exotemplates and other results found in the literature.[13] The calculation of the exact amount of sucrose and its introduction into an exotemplate will be demonstrated in the following section. The optimum nanocasting procedure for the meso-macroporous carbon replica CMI-9 (this nomenclature is given for the sake of clarity and simplicity of the description) was to dissolve 0.69 g of sucrose in a 5 mL acidic solution (pH = 0.5; H_2SO_4), and subsequently 1 g of the exotemplate CMI-7-Zr was added to this solution. After 3 h of stirring, the resultant mixture was dried in a muffle oven at 100 °C for 6 h and then at 160 °C for a further 6 h. The CMI-7-Zr, containing the partially carbonized mass, was added to an aqueous acidic (pH = 0.5; H_2SO_4) solution containing 0.41 g of sucrose. The resultant mixture was dried again as described above. The color of the sample turned dark brown. This powder sample was heated to 950 °C under N_2 for 6 h. The carbon−zirconia composite obtained was washed in 40% HF solution for 56 h to completely dissolve the zirconia exotemplate.

2.2. Textural, Structural, and Hydrophobicity Characterization. The transmission electron microscopy (TEM) micrographs of the carbon replica were taken using a 100 kV Phillips Technaï microscope. Sample powders were embedded in an epoxy resin and sectioned with an ultramicrotome. The morphology of the obtained solid phases was studied using a Philips XL-20 and a Jeol scanning electron microscope. Nitrogen adsorption−desorption isotherms were obtained at −196 °C over a wide relative pressure range from 0.01 to 0.995 with a volumetric adsorption analyzer TRISTAR 3000 manufactured by Micrometrics. The mesopore diameter and the mesopore size distribution were determined by using the Barret−Joyner−Halenda (BJH) method. Although it is well-known that these methods give an underestimated pore size, these methods were used in comparison with other studies that used the same methods. The large mesopore and macropore diameters and their pore size distribution were obtained by Hg porosimetry (Carlo-Erba 2000) using the Washburn relation. Thermogravimetry measurements were performed with a TG/DSC-111 from Setaram. The final carbon material was heated progressively (2 °C/min) until 650 °C under oxidizing conditions to verify that the structure was pure carbon. Fourier transform infrared (FT-IR) spectroscopy (Perkin-Elmer Spectrum 2000) measurements were also carried out to confirm the purity of the final meso-macropoprous carbon material.

3. Results and Discussion

3.1. Properties and Further Characterization of Exotemplates. The synthesis and characterization by N_2 adsorption, TEM, and Hg porosimetry of the starting multimodal porous ZrO_2 exotemplate have been described in detail elsewhere,[35−39] and thus what follows is only a summary of the characteristics of the exotemplate. However, for a better understanding of the synthesis strategy used, new, previously unpublished scanning electron microscopy (SEM) images of the CMI-7-Zr exotemplate, obtained with a higher resolution microscope, are included in Figure 1. The synthesized meso-macroporous zirconia particles exhibit macroscopic network structures with relatively homogeneous and funnel shaped macropores of 100−600 nm in dimension (Figure 1). The macrochannels are arranged parallel to each other and perpendicular to the tangent of the smooth and dense particle shell (Figure 1a−c). The mesoporous walls around the macrochannels are composed of very homogeneous nanoparticles of about 50−70 nm (Figure 1d−f), resulting in an interparticular porosity with 20−30 nm sized voids. These nanoparticles, which for the sake of clarity are herein called secondary particles, themselves possess acces-

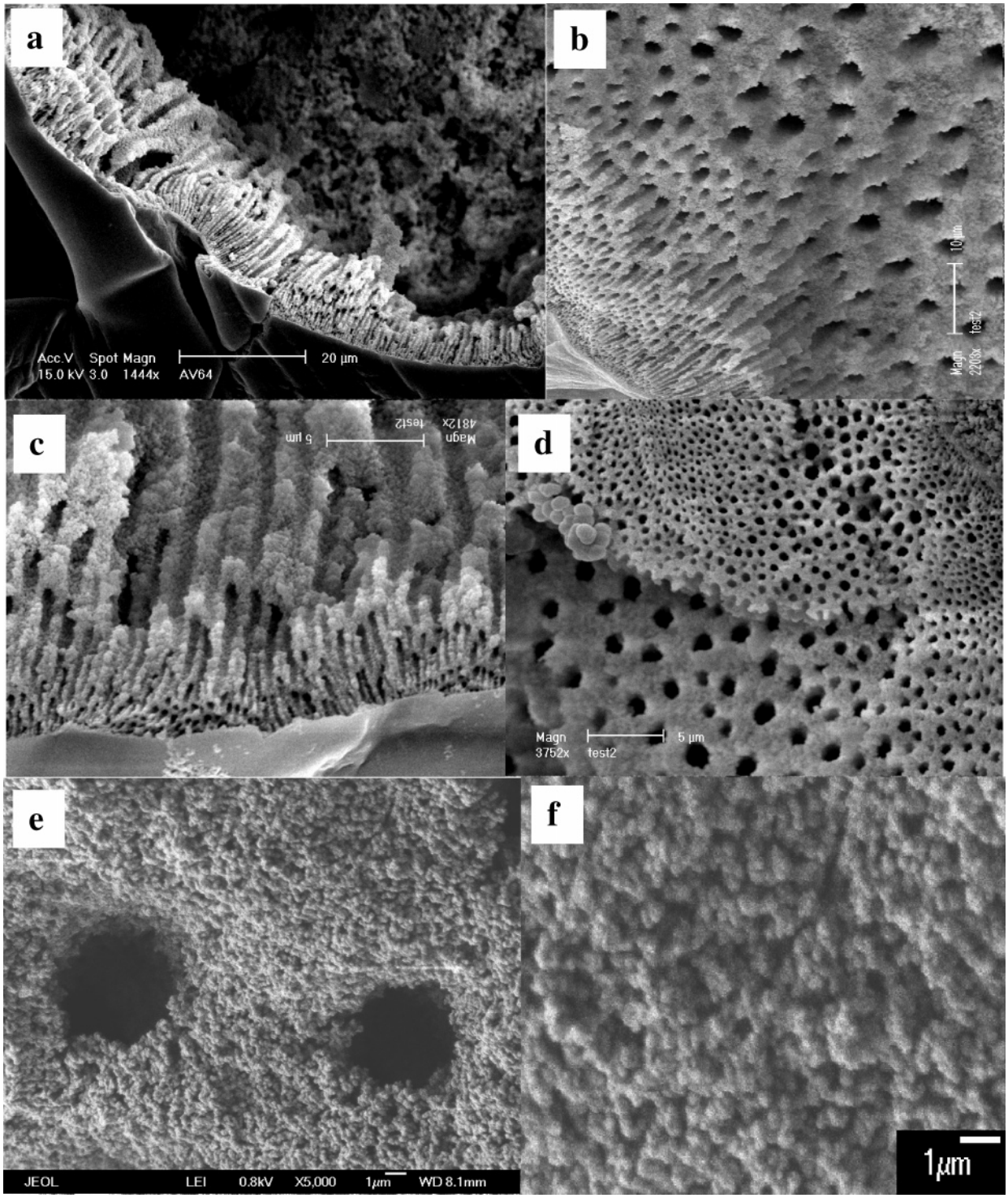

Figure 1. SEM images of meso-macroporous zirconium oxide. Images a, b, and c are side views showing straight parallel macrochannels with a funnel-like shape which are perpendicular to the tangent of the particles' dense mesostructured layer. Images d, e, and f are top views at different magnifications showing the assembly of secondary nanoparticles around the macrochannels (d and e) which are themselves composed of smaller primary nanoparticles (f).

sible mesochannels with a wormhole-like array formed by smaller nanoparticles of several nanometers namely called primary particles (Figure 1f). The synthesized ZrO_2 exotemplate exhibits nitrogen adsorption−desorption isotherms of type IV with a high surface area of 664 m^2 g^{-1} and a mesopore (below 7 nm) volume of 0.42 cm^3/g. The analysis of the pore size distribution by the Barret−Joyner−Halenda method from the adsorption branch of the isotherm reveals a narrow pore size distribution centered at 2.1 nm, which is attributed therefore to the voids formed by the primary nanoparticles (Figure 1f). At relative pressures higher than 0.85, a strong increase in adsorbed nitrogen volume is observed, revealing an appreciable amount of secondary porosity, owing to the large mesopores or the interparticle porosity. This secondary porosity can be attributed to the mesovoids observed in the walls formed by secondary nanoparticles of 50−70 nm. The pore size distribution, determined from mercury intrusion and extrusion curves obtained by the mercury porosimetry, showed that the zirconia particles have macropore diameters in the range of

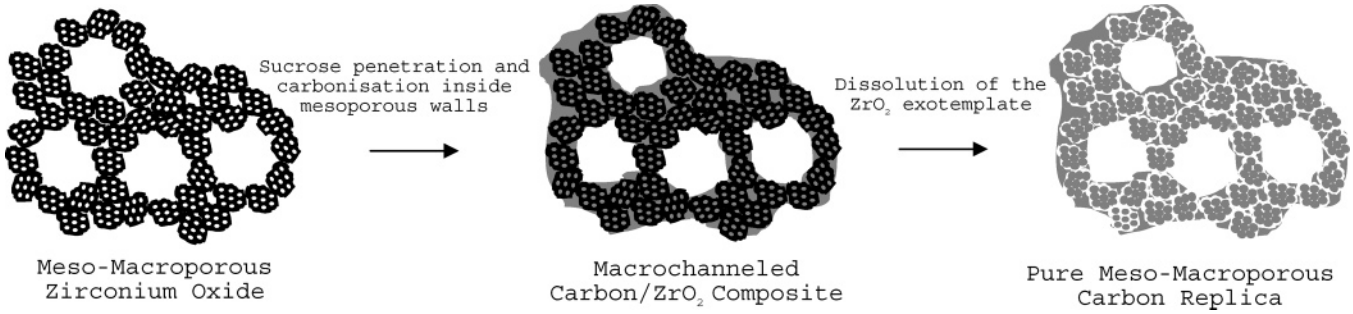

Figure 2. Schematic representation of the new nanocasting method used to synthesize pure meso-macroporous carbons: the replica of mesoporous walls and the transmission of macrochannels from exotemplate to carbon material.

60−700 nm. An interparticular porosity of 10−30 nm is also seen in the zirconia exotemplate. All these techniques reveal that the current material exhibits the trimodal pore structure of a meso-macroporous system. This hierarchy of the zirconia makes it a suitable exotemplate for the preparation of carbon materials possessing a hierarchical meso-macroporous structure with well organized and parallel macrochannels.

3.2. Synthesis: Strategy and Results. As discussed above, there is a great difficulty in synthesizing porous carbon materials with the same architecture as CMI-7-Zr has when using the nanocasting method. One must preserve the macrochannels of the template within the replica. During the replication, all the macrochannels would be filled in by a carbon source. After the removal of the ZrO_2 exotemplate, the macrochannels present in the template remain filled by carbon so would not be transmitted to the final materials. On the basis of this analysis and some recently developed methods,[29−31,34] a new strategy of replication relies on the determination of an appropriate quantity of carbon precursor (sucrose). An amount of sucrose, sufficient only to fill the mesoporous walls separating the macrochannels, will be used, and all the macrochannels thus remain empty. In this way, one can obtain a carbon replica of the mesoporous inorganic walls and always transmit the macrochannels from the exotemplate to the carbon material. Thus, the mesoporous carbon material with the aligned macrochannels identical to those present in the template can be designed as illustrated in the schematic representation (Figure 2). The main aim is to avoid complete filling of the macropores of the exotemplate by limiting the amount of carbon precursor. The macrochannels are coated with carbon to retain them after template removal. This is exactly what was performed in the present study.

Theoretically, about 1.6 g of solid sucrose can be incorporated within a pore volume of 1 cm^3.[13] However, for a successful impregnation, the sucrose must be dissolved in an aqueous solution containing sulfuric acid (ca. 80 wt % in sucrose); therefore, the appropriate quantity of sucrose decreased to 1.25 g. The subsequent heat treatment, carried out at 160 °C, allowing sucrose to decompose, could make the exotemplate take up an additional quantity of sucrose (0.75 g/cm^3), which was experimentally determined on mesoporous silica structures.[13] In other words, a solid with a pore volume of 1 cm^3 can store around 2.0 g of sucrose solution within the pores. In the present case, 1 g of the hierarchically structured meso-macroporous zirconia was used as an exotemplate. Attempts were made to completely and exclusively fill the mesoporous walls that separate the macrochannels which themselves remain empty during the impregnation process. The porous volume of the mesoporous walls is around 0.55 cm^3/g, whereby 0.42 cm^3/g is attributed to the mesopores as determined by N_2 adsorption−desorption,[38] and the remaining 0.13 cm^3/g arises from the interparticular porosity as determined by Hg porosimetry.[38] Thus, 0.69 g followed by 0.41 g of sucrose solution have to be impregnated inside the zirconia exotemplate to give a sucrose solution content of 2 g per 1 cm^3 pore volume. The sucrose located in the mesoporous walls is converted into carbon under N_2 at 950 °C, and the zirconia framework is then removed by dissolution in hydrofluoric acid.

The synthesized carbon particles with a macroscopic morphology identical to the starting zirconia exotemplate are mainly tens of micrometers in size with a regular array of macrochannels, as shown in the SEM images in Figure 3. The tubular macropores, 100−600 nm in diameter, are uniformly distributed within the particles. They are funnel shaped (Figure 3b−d) and perpendicular to the smooth surface of the particle (Figure 3b,d), similar to the macropores of the zirconia exotemplate (Figure 1a−c). The SEM images in parts b, c, and d of Figure 3 show the upper part and lower part of a meso-macroporous carbon particle, highlighting parallel funnel shaped macrochannels open at the top and closed at the dense mesoporous bottom. These are the exact same shape as those observed in the zirconia exotemplate with an identical pore gradient (Figure 1a−c). It can be clearly seen in Figure 3c,e that the macrochannel walls are formed by nanoparticle assemblies despite the low quality of the picture.

The SEM results were corroborated by mercury porosimetry measurements. As shown in Figure 4a, the pore size distribution, calculated from the mercury intrusion and extrusion curves obtained by the mercury porosimetry of the carbon replica, yields the macropore sizes centered at 100−600 nm while the zirconia particles have macropore diameters in the range of 60−700 nm.[38] The slight difference in the macropore sizes is due to a slight shrinkage during the pyrolysis step. The interparticular porosity of ca. 10−30 nm, seen in the zirconia exotemplate,[38] generates two different mesoporosities in the carbon replica with narrower pore size distributions at 15−17 and 25−50 nm. The interparticular mesoporous volume is around 0.13 cm^3/g.

Figure 4b shows the nitrogen adsorption−desorption isotherms and the corresponding pore-size distribution of the synthesized carbon material. The isotherms are of type IV,

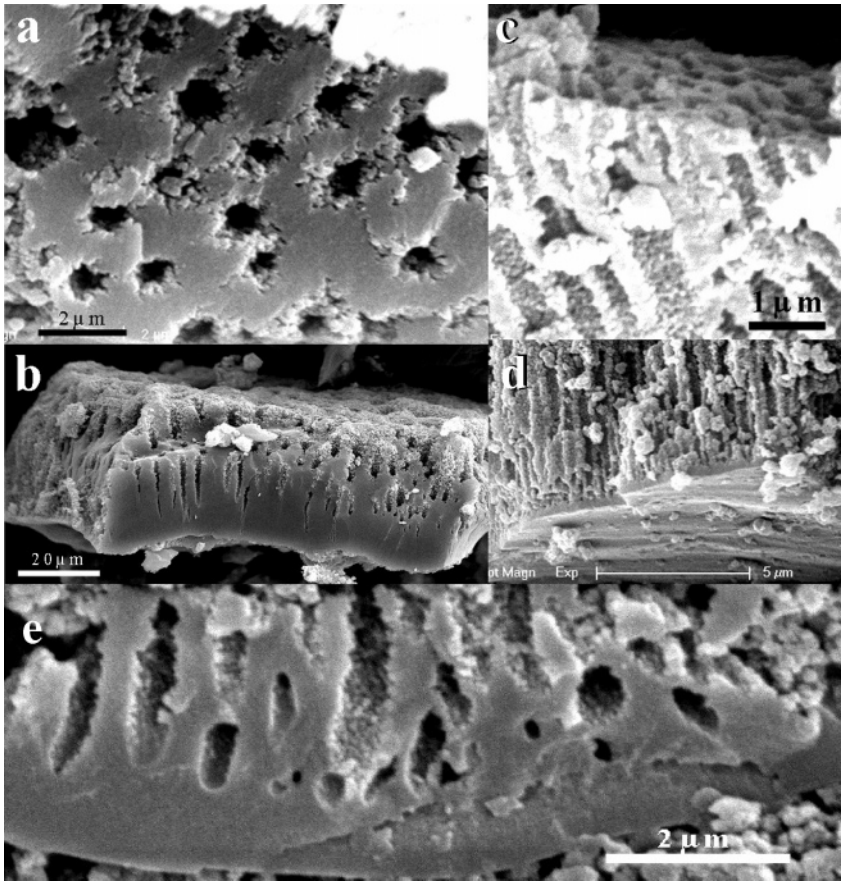

Figure 3. Representative SEM images of the hierarchically structured ordered meso-macrostructured carbon replica.

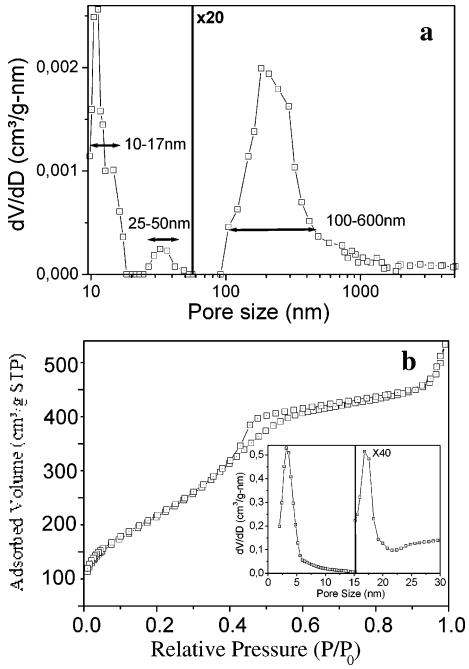

Figure 4. Pore size distribution curves obtained by mercury porosimetry (a) and nitrogen adsorption−desorption isotherms (b) of the synthesized meso-macroporous carbon replica. The inset of b is the corresponding pore size distribution curve calculated from the adsorption branch of the isotherm.

characteristic of mesoporous materials according to the IUPAC classification system. The hysteresis loop appears to be of type H2, indicating that the material has good pore connectivity, with channel-like or ink-bottle pores. Two pore-size distributions are obtained, one centered at 3.0 nm, which is slightly broader than that of the zirconia exotemplate,[38] and another at 15−17 nm, confirming the Hg porosimetry measurements. As a result of the technical limitation of N_2 adsorption and the low amount of pores around 20−25 nm detected by Hg porosimetry, a pore size distribution in this range cannot easily be determined. While at relative pressures higher than 0.90, the adsorbed volume of nitrogen increased significantly, which suggests that the carbon material contains an appreciable amount of large pores in the macropore range. A very high surface area of 950 m^2/g with a mesopore volume of 0.44 cm^3/g was obtained.

The macroporosity of the carbon replica was further confirmed by TEM observations of the microtomed carbon specimen (Figure 5). The well-defined macroporous structure can clearly be seen with the macropore sizes being in accordance with SEM and Hg porosimetry results. The wall thickness between the circular openings of macropores is about 100−500 nm. High-magnification TEM images reveal a disordered wormhole-like mesoporous structure within the walls (Figure 5d). The presence of a significant amount of mesopores in the range of 15−17 and 25−50 nm can be clearly visualized in the TEM picture (Figure 5b). These results demonstrated that although the ZrO_2 exotemplate was impregnated by sucrose solution acidified with H_2SO_4, a strong acid, no structural damage to the ZrO_2 porous exotemplate occurred. The carbon materials represent a positive replica of the starting ZrO_2 porous exotemplate with similar sized macrochannels while the volume templated mesopores within the dense shell of the particles and the

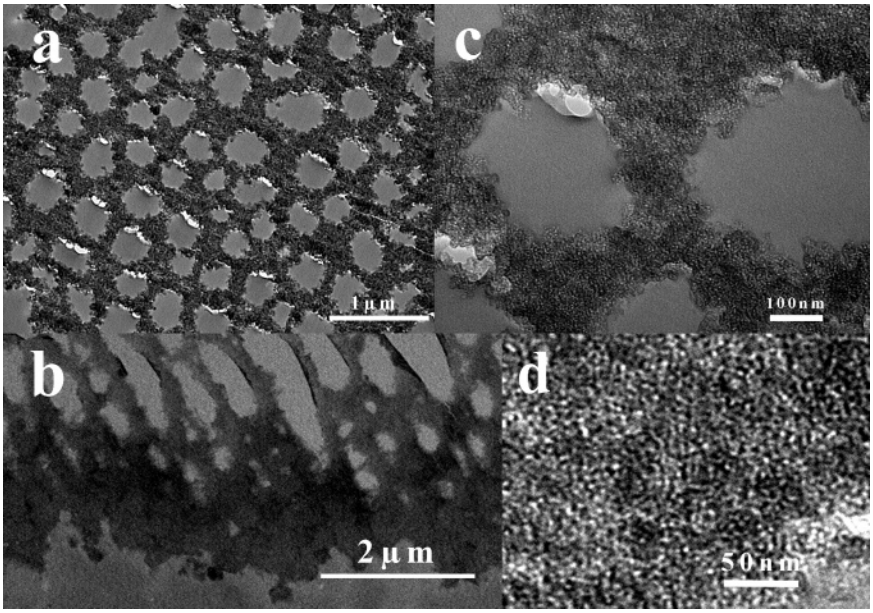

Figure 5. Cross-sectional TEM images of the synthesized meso-macroporous carbon material. Images a and b are the low-magnification micrographs of the macropores viewed perpendicular (a) and side-on (b) to the pores, respectively. Image c is a higher magnification micrograph of image a. Image d is a high-resolution TEM image showing the disordered mesoporous walls of macropores.

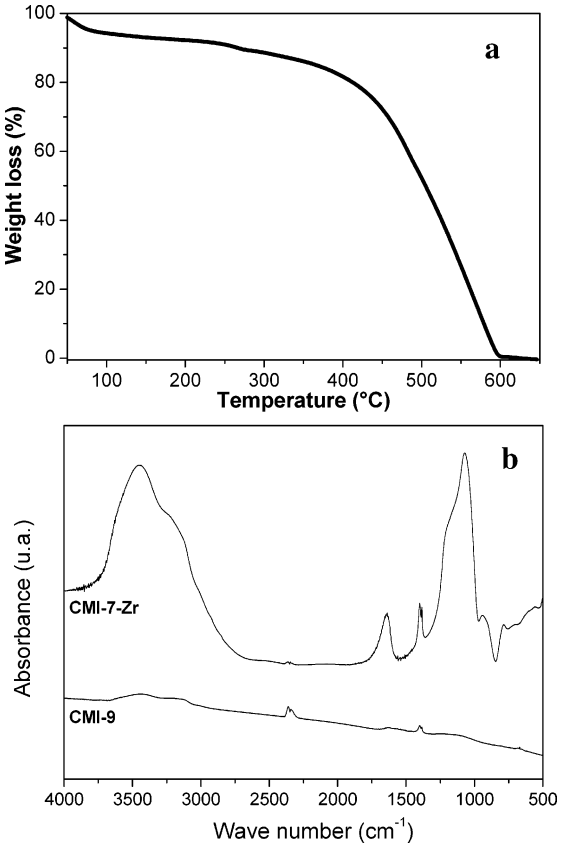

Figure 6. Thermogravimetry curve (a) of the CMI-9 meso-macroporous carbon and FT-IR spectra (b) of the meso-macroporous zirconia exotemplate and CMI-9 carbon replica.

walls of the macrochannels are a negative replica of the ZrO_2 exotemplate.

The purity of the carbon material was studied by thermogravimetric and FT-IR measurements (Figure 6). The thermogravimetric measurements (Figure 6a) under air show that the carbon material begins to combust around 400 °C and disappears completely around 610 °C. Less than 1% of the exotemplate remains at this temperature (610 °C), indicating an almost pure carbon framework. The minimal loss in weight at temperatures below 100 °C indicates that practically no water molecules are present in the pores of the porous carbon material. The FT-IR spectrum of the carbon replica (Figure 6b) confirms the purity highlighted by thermogravimetry. It is interesting to note that, in the IR spectrum of the zirconia exotemplate (Figure 6b), a very intense and broad band in the range of 2700−4000 cm^{-1} and another intense band in the range of 1400−1600 cm^{-1} are found. These arise because of the physisorbed water molecules within the pores, revealing the hydrophilicity of the exotemplate material. The first band is greatly reduced in intensity such that only a very weak band is slightly visible in the IR spectrum of the carbon materials. However, the second band is not found which suggests that, in stark contrast to the exotemplate, the carbon materials are essentially hydrophobic. The strong band in the range of 800−1300 cm^{-1}, observed in the spectrum of the ZrO_2 exotemplate, is due to the vibration of the framework ZrO_4 species. This too completely disappears in the spectrum of the carbon replica, indicating the complete removal of the ZrO_2 exotemplate and thus pure the carbon composition of the final carbon replica. Both the strong hydrophobicity and the high purity of the obtained meso-macroporous carbon material were evidenced by these two techniques.

The effect of the amount of sucrose impregnated inside the meso-macroporous zirconia exotemplate on the nanoreplication was also studied. The investigations about the exact amount of sucrose to use were based on the global textural properties of the zirconia exotemplate, which were obtained by nitrogen adsorption−desorption and Hg porosimetry techniques. When less than 2 g of sucrose solution (ca. 80 wt %) per 1 cm^3 pore volume was added, no macropores were obtained. The synthesized carbon particles were smaller than 1 μm and only mesostructured (Figure 7a). This indicates that the amount of sucrose was

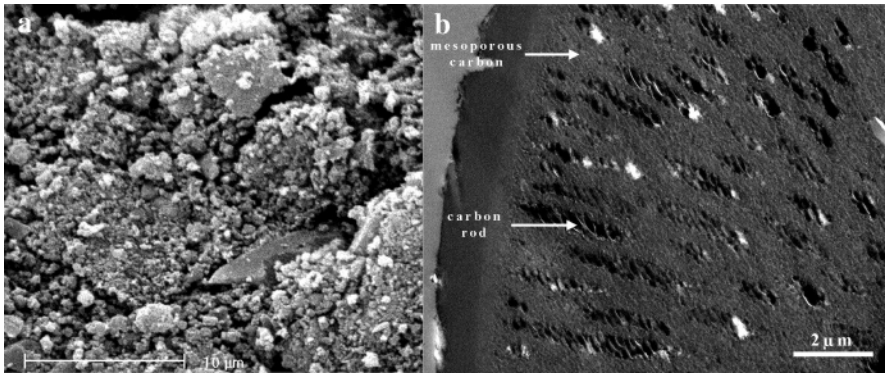

Figure 7. SEM picture (a) of carbon material obtained from a material with an amount of sucrose less than 2 g/1 cm^3 pore volume. The amount of sucrose impregnated is insufficient to fill the mesoporous system. TEM picture (b) of carbon material obtained after a very high sucrose loading which completely filled the mesoporous walls (mesopores and interparticular pores) and macrochannels of the exotemplate.

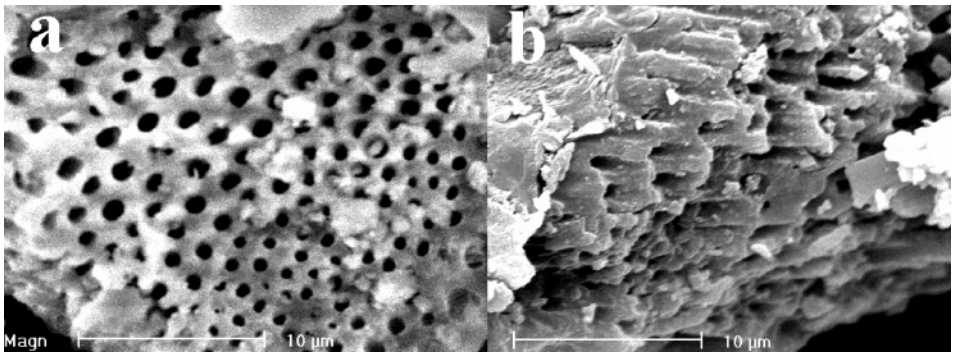

Figure 8. SEM images of (a) the meso-macroporous aluminosilicates and (b) the corresponding carbon replica.

notsufficient to completely fill in the mesoporous walls to yield a continuous carbon structure, which in turn leads to the collapse of the meso-macroporous structure after removal of the ZrO_2 exotemplate. When more than 2 g of sucrose solution (ca. 80 wt %) per 1 cm^3 pore volume was impregnated inside the exotemplate, the mesopores in the primary nanoparticles and the interparticular pores as well as the macrochannels were all completely filled by sucrose. The carbon particles obtained were approximately 10 μm. These particles were composed of dense carbon rods with diameters of around 100−600 nm, surrounded by a mesoporous envelope, leading to the formation of dense carbon material. However, the rods contain micropores generated by the removal of oxygen and hydrogen from the sucrose (Figure 7b). The macrochannel system was lost. This figure also shows three zones with different contrasts. First, outer layer of the particle has a thickness of approximately 1.0−1.5 μm. It can be distinguished from the mesoporous envelope as it is distinctly darker owing to the relatively high density of carbon in this zone. This density arises from the infiltration of sucrose within a dense layer of the ZrO_2 exotemplate containing small mesopores. The darkest part in the form of rods is due to the complete and dense infiltration and carbonization of the carbon precursor in the macrochannels. These carbon rods can be identified in the TEM image as the darkest regions of the picture. During the preparation of the TEM sample by the microtoming technique, it was observed that there was a significant resistance when cutting the samples. This suggests the existence of denser regions within the particle. The rest of the particle, labeled mesoporous carbon in the image, is a lighter shade as this region is less dense owing to the high porosity after the removal of the exotemplate. The infiltration was made only in the large interparticular voids. After the removal of ZrO_2 exotemplate, this part is quite porous with low density and, thus, less dark.

This study shows that to keep the macrochannel system, only the mesopores must be filled by the sucrose while the macrochannels must remain empty during the nanoreplication. This is the key point to the success in the preparation of hierarchical multimodal meso-macroporous carbon materials with straight and parallel funnel-like macrochannels.

Furthermore, the nanoreplication of other meso-macroporous oxides, such as aluminosilicates, titania, and niobia, used as examples for host scaffolds, have also been investigated by a similar process described herein. Well aligned macrochannels identical to the exotemplate can be clearly visualized by SEM image in Figure 8.

4. Conclusion

A new kind of mesoporous carbon with funnel shaped macrochannels has been synthesized by the exotemplating process. This method is successful owing to the fine-tuning of the amount of sucrose impregnated within a meso-macroporous metal oxide exotemplate. This allows the replication of only the mesoporous walls, with the macrochannels left empty. The macrochannels in the exotemplate are therefore preserved and transmitted to the carbon material. The synthesized meso-macroporous carbons are suitable

candidates for applications in areas where a hierarchical porosity, producing a combination of efficient transport and high surface area, is of great importance. Examples include separation and purification processes and also biological applications. They can also be used to remove volatile organic compounds (VOCs), odorous molecules or dioxins and furans from air and water by adsorption or as catalyst supports for various reactions. New advances achieved in the synthesis of novel types of meso-macroporous carbon materials are providing opportunities for the large scale fabrication of carbon membranes. It is also expected that this facile synthesis method would be suitable for obtaining other carbon macrochannels with mesoporous walls by using other hierarchically structured meso-macroporous metal oxide exotemplates.

Acknowledgment. This work was supported by the Inter-university Attraction Poles Program (P6/17)-Belgian State-Belgian Science Policy and the European Program of InterReg III (Programme France-Wallonie-Flandre, FW-2.1.5). A FRIA (Fonds National de la Recherche Scientifique, Belgium) doctoral scholarship program for A.V., the financial support from the Walloonia Region Government (Belgium), and the correction in the text by Dr. Z. Y. Yuan and in English by Dr. J. Rooke are also acknowledged.

CM070294O